SGP-TR-147-36

PROCEEDINGS

NINETEENTH WORKSHOP
GEOTHERMAL RESERVOIR ENGINEERING

January 18-20, 1994

Henry J. Ramey, Jr., Roland N. Horne,
Paul Kruger, Frank G. Miller,
William E. Brigham, Jean W. Cook
Stanford Geothermal Program
Workshop Report SGP-TR-147

DISCLAIMER

PROCEEDINGS, Nineteenth Workshop on Geothermal Reservoir Engineering
Stanford University, Stanford, California, January 18-20, 1994
SGP-TR-147

THEORETICAL STUDIES OF FLOWRATES FROM SLIMHOLES AND PRODUCTION-SIZE GEOTHERMAL WELLS

Teklu Hadgu, Robert W. Zimmerman and Gudmundur S. Bodvarsson

Earth Sciences Division
Lawrence Berkeley Laboratory
University of California
Berkeley, CA 94720

ABSTRACT

The relationship between production rates of large diameter geothermal production wells, and slimholes, is studied. The analysis is based on wells completed in liquid-dominated geothermal fields, where flashing occurs either in the wellbore or at the surface. Effects of drawdown in the reservoir, and pressure drop in the wellbore, are included; heat losses from the wellbore to the formation are not presently included in our analysis. The study concentrates on the influence of well diameter on production rate. For situations where the pressure drop is dominated by the reservoir, it is found that the mass flowrate varies with diameter according to $W \sim D^{\alpha}$, where the exponent α is a function of reservoir outer radius, well diameter and skin factor. Similarly, when pressure drop in the wellbore is dominant, the scaling exponent was found to be a function of well diameter and pipe roughness factor. Although these scaling laws were derived for single-phase flow, numerical simulations showed them to be reasonably accurate even for cases where flashing occurs in the wellbore.

INTRODUCTION

Drilling of slimholes instead of large diameter production-sized wells may be economically beneficial during the exploration phase of a geothermal prospect or during exploration of an undeveloped part of a producing reservoir. It has been reported that slimholes with diameters less than or equal to 4" could reduce the cost and time of drilling significantly (see for example, Entingh and Petty, 1992). Slimholes can also provide continuous cores which would help identify geological features more clearly. This report concentrates on the effect of wellbore diameter on production characteristics. Cost analysis, drilling practices and other relevant topics concerning slimholes are not discussed.

As fluid flows from the reservoir to the surface through the wellbore, pressure drawdown occurs both in the reservoir and in the wellbore. As pointed out by Pritchett (1993), it would be helpful to have a scaling law that allows the flowrate of a slimhole to be predicted from the flowrate of a normal-diameter hole under the same conditions. Following Pritchett, we will attempt to develop power-law scaling relationships to describe the effect of wellbore diameter on well output. We first carry out an analysis for single-phase flow, for which it is possible to derive some analytical expressions. We then discuss the case where flashing occurs at some point in the wellbore.

PRESSURE DRAWDOWN IN THE RESERVOIR

Fluid flow from the reservoir into the wellbore has been studied by many investigators over the last half century or so, including processes such as the nature and direction of flow, transient or steady-state, single or two-phase, laminar or turbulent flow, and permeability reduction (well damage) or enhancement due to drilling and production/injection activities.

In these studies, reasonable simplifications have been suggested. For instance, the flow from the reservoir into the wellbore is sometimes assumed to be steady or quasi-steady, because flow equilibrates faster near the wellbore than in the reservoir as a whole (Pritchett and Garg, 1980). One could consider the direction of flow into the wellbore as spherical. However, with time it is assumed to approach horizontal radial flow. Other assumptions can also be made based on estimates of the amount and type of fluid, and the near-well reservoir behavior.

Consider the pressure drop that occurs in the reservoir as the fluid flows toward the wellbore. Imagine a bounded, circular reservoir, whose outer boundary $r = r_o$ is maintained at some pressure p_o (see Fig. 1). If the wellbore has radius r_w, and the downhole wellbore pressure is maintained at p_{wb}, the steady-state flowrate under Darcy-flow conditions will be given by (Matthews and Russell, 1967, p. 21)

$$W = \frac{2\pi\rho kh}{\mu}\,\frac{(p_o - p_{wb})}{\ln(r_o/r_w) + s} \qquad (1)$$

where ρ is the fluid density, kh is the reservoir permeability-thickness product, μ is the fluid viscosity, and s is the well skin factor. This relation between pressure drop and flowrate will also hold during the transient process of production from a reservoir that is initially at uniform pressure, except at extremely small times that are of little practical relevance (see de Marsily, 1986, pp. 161-167). Hence, this relation is sufficiently general that it can be used as the basis of our scaling-law analysis. Equation (1) is often written in terms of the productivity index as

$$W = \frac{\rho PI}{\mu} (p_o - p_{wb}) \qquad (2)$$

where PI is the productivity index, which can be expressed as

$$PI = \frac{2\pi kh}{\ln(r_o/r_w)+s} \qquad (3)$$

If we compare two wells of different diameters that are producing under otherwise identical conditions, equations (1) and (3) predict that their flowrates will be in the ratio

$$\frac{W_1}{W_2} = \frac{PI_1}{PI_2} = \frac{\ln(2r_o/D_2)+s_2}{\ln(2r_o/D_1)+s_1} \qquad (4)$$

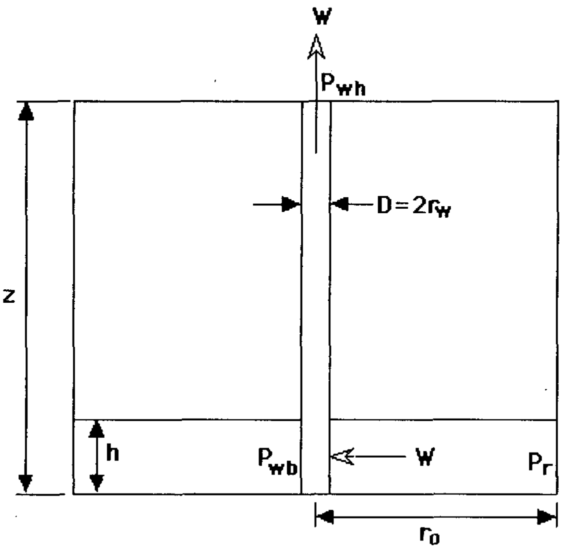

Fig. 1. Schematic diagram of the problem considered.

This ratio depends on the wellbore diameters, and also on the outer radius of the reservoir. In order to simplify the analysis that follows, we will assume that the skin factor does not depend on diameter, i.e., $s_1 = s_2$. However, if there was some knowledge of the variation of s with D, the method described below could be modified to account for this. For simplicity, and because power-law equations (representing different effects) can easily be combined, we will approximate equation (4) with a power-law. If $(PI_1/PI_2) = (D_1/D_2)^\beta$, then the exponent β would be given by

$$\beta = \frac{d\ln PI}{d\ln D} = \frac{D}{PI}\frac{dPI}{dD}. \qquad (5)$$

In order to fit equation (4) to a power-law equation, we take its logarithmic derivative as in equation (5), and evaluate it at some reference diameter D_2. Specifically, we treat the parameters with subscript 1 as variables, and hold those with subscript 2 constant, and then set $D_1 = D_2$ when evaluating the derivative, to arrive at

$$\left.\frac{D}{PI}\frac{dPI}{dD}\right]_{D_1=D_2} = \beta = \left[\ln\left[\frac{2r_o}{D_2}\right] + s\right]^{-1} \qquad (6)$$

Hence the ratios of the productivity indices and flowrates, between two otherwise identical boreholes, each having the same pressure drawdown in the reservoir, will be

$$\frac{W_1}{W_2} = \frac{PI_1}{PI_2} = \left[\frac{D_1}{D_2}\right]^{[\ln(2r_o/D_2)+s]^{-1}} \qquad (7)$$

To estimate the ratio of mass flowrates, the outer radius r_o and the skin factor s have to be determined. The skin factor may be obtained from well test analyses. For reservoir modeling exercises r_o is the distance to the nodal point of the wellblock, the value of which depends on the type of computational grid selected. Hadgu et al. (1993) recently presented a method for determining the distance from the well to the nodal point of the wellblock. Similar studies have also been reported by Aziz and Settari (1979) and Pritchett and Garg (1980), among others.

If non-Darcy flow effects are important, equation (2) becomes inadequate; an analysis of this situation is given by Hadgu et al. (1993), Kjaran and Eliasson (1983), Hadgu (1989), Iglesias and Moya (1990) and Gunn and Freeston (1991), among others.

PRESSURE DROP IN THE WELLBORE

The pressure drop in the wellbore is a sum of frictional, gravitational and accelerational components. For convenience, the following analysis ignores the accelerational pressure drop. For a comparison of output of large and small diameter wells, the parameters of interest will be friction factor λ, mass flowrate W, and the inside pipe diameter D.

First, consider the flow in the wellbore, temporarily ignoring the pressure drop in the reservoir itself. Under the assumption that the dynamic properties and pressure drop are the same for two wells with diameters D_1 and D_2, Pritchett (1993) proposed the following scaling law based on the ratios of the cross-sectional areas:

$$\frac{W_1}{W_2} = \frac{A_1}{A_2} = \left[\frac{D_1}{D_2} \right]^2 \quad (8)$$

A more accurate scaling equation in the form of a power-law can be formulated by considering the equations that govern wellbore flow, including the effect of frictional losses. The frictional and gravitational components of the pressure gradient can be expressed as

$$\frac{dp}{dz} = \left[\frac{dp}{dz}\right]_{fric} + \left[\frac{dp}{dz}\right]_{grav} = \frac{\lambda \rho v^2}{2D} + \rho g \quad (9)$$

where λ is the Darcy friction factor and v is the mean fluid velocity, which is equal to $W/(\pi D^2/4)$. If we are comparing flows in two wellbores that occur under the same pressure drop, and assuming equivalent fluid properties, then equation (9) reduces to

$$\frac{\lambda v^2}{D} = \frac{2}{\rho}\left[\frac{dp}{dz} - \rho g\right] = \text{constant} = C \quad (10)$$

The friction factor depends on the Reynolds number, which is defined by

$$Re = \rho v D/\mu \quad (11)$$

as well as on the relative roughness of the wellbore casing, ε/D. One correlation that has been widely used to relate these parameters is the Colebrook equation (White, 1974, p. 498):

$$\frac{1}{\sqrt{\lambda}} = 1.74 - 4.605 \ln\left[\frac{2\varepsilon}{D} + \frac{18.7}{R_e\sqrt{\lambda}} \right] \quad (12)$$

In order to find a relationship between flowrate and diameter, we first use equations (11) and (12) to eliminate explicit reference to Re and λ, to find

$$v = (CD)^{0.5}\left[1.74 - 4.605 \ln\left[\frac{2\varepsilon}{D} + \frac{18.7\mu}{\rho\sqrt{C}\, D^{1.5}}\right]\right]$$
$$\equiv (CD)^{0.5} f(D) \quad (13)$$

The first part of the right-hand side of the expression is already in the form of a power-law equation. The bracketed term f(D) is not of that form, but can be approximated by a power-law. If we assume

$$f(D) = \text{const. } D^{\alpha} \quad (14)$$

the parameter α would be given by

$$\alpha = \frac{d\ln f}{d\ln D} = \frac{D}{f}\frac{df}{dD} \quad (15)$$

We can calculate the derivative df/dD, and then evaluate expression (15) at some reference value $D = D_2$, to arrive at a value for the scaling exponent α. Carrying out this differentiation, and then expressing the results in terms of Re and λ, we eventually find

$$\alpha = 4.605\sqrt{\lambda_2}\left[\left(\frac{2\varepsilon}{D_2} + \frac{18.7(1.5)}{Re_2\sqrt{\lambda_2}}\right) \Big/ \left(\frac{2\varepsilon}{D_2} + \frac{18.7}{Re_2\sqrt{\lambda_2}}\right)\right] \quad (16)$$

Equation (16) has a very weak dependence on Re, since the bracketed term varies only from 1, at high Reynolds numbers, to 1.5, at low Reynolds numbers. Hence, in order to arrive at a value of α that depends on as few parameters as possible, we now evaluate equation (16) in the limit of high Reynolds numbers. In this case, the bracketed term in equation (16) goes to 1.0, and for realistic values of ε/D, equation (12) can be approximated by

$$\sqrt{\lambda_2} = \left[- 4.605 \ln(2\varepsilon/D_2)\right]^{-1} \quad (17)$$

Equation (16) then simplifies to

$$\alpha = -\left[\ln\left(\frac{2\varepsilon}{D_2}\right)\right]^{-1} \quad (18)$$

which depends only on the relative roughness of the casing. If we now combine equations (12, 13 and 14), we find

$$\frac{v_1}{v_2} = \left[\frac{D_1}{D_2} \right]^{0.5 - [\ln(2\varepsilon/D_2)]^{-1}} \quad (19)$$

Finally, we note that the flowrate is given by the product of the mean velocity and the cross-sectional area, so that

$$\frac{W_1}{W_2} = \frac{v_1 A_1}{v_2 A_2} = \frac{v_1}{v_2}\left[\frac{D_1}{D_2}\right]^{2.0} = \left[\frac{D_1}{D_2}\right]^{2.5 - [\ln(2\varepsilon/D2)]^{-1}} \quad (20)$$

If we assume typical values for the relative roughness in the range of 10^{-3} - 10^{-6}, we find that the exponent in equation (20) depends weakly on roughness, and equals about 2.62 ± 0.05. For example, a relative roughness $\varepsilon/D_2 = 10^{-6}$ leads to an exponent of 2.58, whereas a value of $\varepsilon/D_2 = 10^{-3}$ gives an exponent of 2.66. This variation is probably less than the error introduced by fitting equation (13) with a power-law equation. Hence, taking into account the approximate nature of this analysis, one arrives at the following scaling law, which does not contain any reference to the roughness parameter:

$$\frac{W_1}{W_2} = \left[\frac{D_1}{D_2} \right]^{2.62} \quad (21)$$

The exponent 2.62 is close to the value of 2.56 that Pritchett (1993) found by fitting a power-law curve to numerically-computed values of W and D, assuming a wellhead pressure of 1 bar.

TOTAL PRESSURE DRAWDOWN

Assuming that the reservoir pressure (p_r) and the depth of the well (z) are known (Fig. 1), for a selected wellhead pressure (p_{wh}), the sum of pressure drops in the reservoir and in the wellbore, as fluid flows to the surface, can be written as

$$p_r - p_{wh} = \Delta p_{res} + \Delta p_{well} \qquad (22)$$

Using the deliverability equation (2), and assuming a linear drawdown relationship in the reservoir:

$$\Delta p_{res} = \frac{W\mu}{\rho PI} \qquad (23)$$

Pressure drop in the wellbore is subdivided into its components of friction, gravity and acceleration. For single-phase isothermal flow the acceleration term may be ignored. Thus,

$$\Delta p_{well} = \Delta p_{fric} + \Delta p_{grav} \qquad (24)$$

where Δp_{fric} and Δp_{grav} are the frictional and gravitational pressure drops in the wellbore, respectively. These components are further defined by:

$$\Delta p_{fric} = -\frac{\lambda \rho v^2}{2D} z \qquad (25)$$

$$\Delta p_{grav} = -\rho g z \qquad (26)$$

Equation (25) can be written in terms of mass flowrate instead of velocity, using the relationship

$$v = \frac{W}{\rho A} = \frac{4W}{\rho \pi D^2} \qquad (27)$$

Thus:

$$\Delta p_{fric} = -\frac{8z\lambda W^2}{\pi^2 \rho D^5} \qquad (28)$$

Substituting for the individual parameters, equation (22) can be written as:

$$p_r - p_{wh} = \frac{W\mu}{\rho PI} + \frac{8\lambda z W^2}{\pi^2 \rho D^5} + \rho g z \qquad (29)$$

Equation (29) indicates that the parameters which mainly affect pressure drop between the reservoir and the wellhead are discharge rate, productivity index, well depth and diameter, friction factor and fluid properties. If we assume isothermal flow both in the reservoir and in the wellbore, fluid properties will be approximately constant. For a comparison of output of large and small diameter casings, well depth can also be assumed to be constant. Thus, the parameters involved in the comparison of large and small diameter casings will be discharge rate, productivity index, friction factor and well diameter.

Equation (29) can now be rewritten in terms of W and D, with the help of equations for PI and λ. Note that λ is in fact a function of W, as implicitly shown in equation (12), which implies that equation (29) is not simply a quadratic for W. However, we have found that for high Re, λ can be approximated by equation (17), with little loss of accuracy. With this approximation, we can rearrange equation (29) as:

$$\frac{8\lambda z}{\pi^2 \rho D^5} W^2 + \frac{\mu}{\rho PI} W + (\rho g z - p_r + p_{wh}) = 0 \qquad (30)$$

with λ given by equation (17). Equation (30) is a quadratic equation for W which is easily solved. The positive root in the solution for W must be taken, since W is by definition a positive quantity. The following is an example to study the relationship between mass flowrate and diameter for single-phase isothermal flow.

Example 1: A well completed in a liquid dominated geothermal reservoir, where the boundary conditions are chosen so that flashing occurs at the surface. If heat exchange with the rock formation is ignored, this is essentially a case of isothermal liquid flow. The reservoir and wellbore parameters are given in Table 1.

Table 1: Reservoir and Wellbore data for Examples 1 and 2.

	Example 1	Example 2
reservoir pressure p_r (bar)	100	90
reservoir temp. T_r (°C)	160	241
wellhead pressure p_{wh} (bar)	7	7
outer radius r_o (m)	88	88
well depth z (m)	1000	1000
reference diameter D_2 (m)	0.1	0.1
pipe roughness ε (m)	4.5×10^{-5}	4.5×10^{-5}

Equation (30) was then used to solve for W in terms of D and kh. Fig. 2 shows the calculated values plotted as a ratio of mass flowrates vs. the ratio of diameters at different values of permeability-thickness product, using $D_2 = 0.1$ m as the reference diameter. The curve for kh = 100 D-m in Fig. 2, for example, contains straight line sections at low and high values of D_1/D_2. For small values of D_1, the pressure drop is dominated by the wellbore, and the curve follows equation (21). For larger values of D_1, there is less frictional pressure drop in the wellbore, and the pressure drop in the reservoir becomes relatively more important. In this region the curves approach asymptotes where slopes are given by equation (7). In the present example, s

= 0, D_2 = 0.1 m, and r_o = 88 m, so that the exponent in the equation is 0.134.

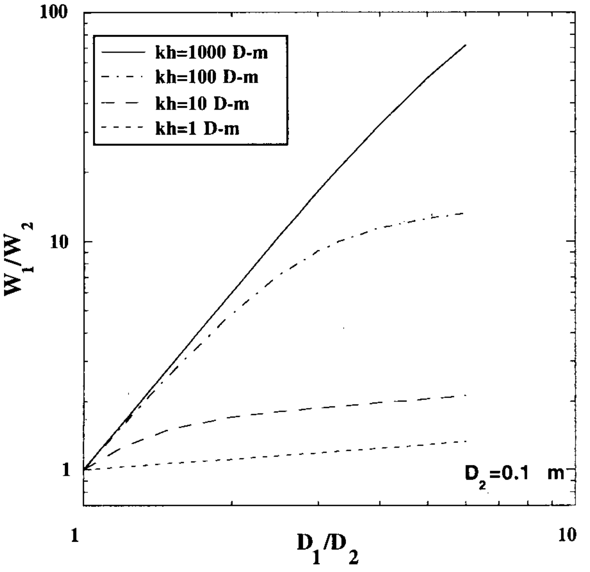

Fig. 2. Ratio of mass flowrate against diameter ratio, for different kh values, for single-phase isothermal flow (see Example 1).

TWO-PHASE FLOW IN THE WELLBORE

If the heat exchange between the wellbore and the surrounding rock formation is important, or two-phase flow exists in the reservoir or wellbore, changes in fluid properties become important. Thus, for non-isothermal single-phase or two-phase flow, fluid properties in the wellbore are not constant, and they have to be integrated over the length of the wellbore. In this case, equation (29) has to be written in the following form:

$$p_r - p_{wh} = \frac{W\mu_r}{\rho_r PI} + \frac{8W^2}{\pi^2 D^5}\int\frac{\lambda(\varepsilon/D,Re)}{\rho}\,d\zeta + g\int\rho\,d\zeta \qquad (31)$$

where ρ_r and μ_r are the density and viscosity at reservoir conditions, ζ is a variable representing depth increment, and the integral is taken from $\zeta = 0$ to $\zeta = z$. Following is an example for two-phase flow.

Example 2: A well is open to a liquid-dominated geothermal reservoir, and flashing occurs in the wellbore. For this example heat exchange with the rock formation is ignored. The reservoir and wellbore parameters assumed are given in Table 1.

The wellbore simulator WFSA (Hadgu and Freeston, 1990) was used to solve for W in equation (31) in terms of D and kh. An iterative scheme was needed to equate the flow in the reservoir to that in the wellbore. Fig. 3 shows the calculated ratio of mass flowrates vs. the ratio of diameters at different values of kh. In this case the effect of fluid properties is evident, as fluid flashes at greater depths, longer columns of two-phase flow result. In Fig. 3, the plots for the higher kh values (i.e. 100, 10 and 1 D-m) show straight line portions for low D_1/D_2 values. This is similar to that of single phase flow where wellbore flow dominates.

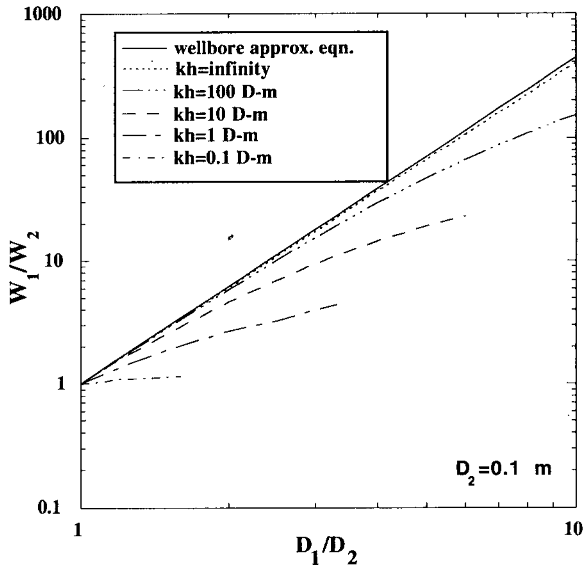

Fig. 3. Ratio of mass flowrate against diameter ratio for different kh values, with flashing occurring in the wellbore (see Example 2).

In this example the wellhead pressure is 7 bars, the undisturbed reservoir pressure is 90 bars, and the saturation pressure at the reservoir temperature of 241°C is 34 bars. Hence flashing will occur at some point between the reservoir far-field and the wellhead. As the wellbore diameter increases, the flow resistance in the wellbore decreases, and flashing occurs deeper. At some critical diameter D* flashing occurs at the bottom of the wellbore, when the bottomhole pressure equals the saturation pressure at the reservoir temperature. If the bottomhole pressure is reduced below the saturation temperature, flashing would occur in the reservoir. Our analysis does not include such cases since equation (31) assumes that fluid properties are constant in the reservoir. For flashing occurring both in the reservoir and in the wellbore a coupled numerical simulation of the flow processes in the reservoir and in the wellbore will be required. Hence our analysis, using equation (31), cannot be used to find the production curve when D is greater than D*.

Density changes also affect the pressure gradients, and the gravitational pressure gradient, which was constant in the single phase case, becomes important. At low flows and large wellbore diameters, the effect of frictional pressure gradient decreases, and the total pressure drop becomes dominated by gravity and reservoir drawdown.

The above analysis was made using the total pressure drawdown. The same parameters were also used to compare the pressure drop in the wellbore (i.e., no reservoir drawdown) with that of single-phase flow, by using equation (31) without the reservoir term. In order to evaluate the integral appearing in equation (31), we need to know how the density varies as a function of depth. To find the density profile, we use the wellbore simulator WFSA, which in effect performs the required integrations. The production rate, shown in Fig. 3 as the curve labeled k = infinity, is then compared with that produced by equation (20), which was developed for single-phase flow. The results are shown in Fig. 3, where it is seen that these two curves are quite close to each other, suggesting that equation (20) may also be used for some cases where flashing occurs in the wellbore.

For reservoir management purposes, it is useful to have plots of mass flowrate as a function of wellhead pressure, for given wellbore diameter values. Such production curves are shown in Fig. 4, for the case described in Example 2. In this case the wellhead pressure was not held constant. Equation (31) was used to compute values of W and p_{wh} at constant diameter and kh. Fig. 4 shows the characteristic curves obtained for different diameters at a constant kh of 100 D-m. Note that the curves are identically shaped, but are displaced vertically on a semi-log plot; this can be explained as follows. For the parameters used in this example, kh is relatively high, and most of the flow resistance occurs in the wellbore. Hence, we see from equations (10) and (21) that

$$W(D) = f(p_{wh})\,(D/D_2)^{2.62} \tag{32}$$

so that

$$\begin{aligned} \log(W(D)) &= \log(f(p_{wh})) + 2.62\log(D/D_2) \\ &= F(p_{wh}) + 2.62\log(D/D_2) \end{aligned} \tag{33}$$

Hence each curve should have the same shape, given by the function $F(p_{wh})$, but with a vertical offset equal to $2.62\log(D/D_2)$. As an example, consider the curve for D = 0.2 m, for which $D/D_2 = 0.2/0.1 = 2$. The calculated offset of 2.62log(2) = 0.79 is shown as a vertical line in Fig. 4, where it is seen to be very nearly equal to the actual vertical offset between the D = 0.2 m and D = 0.1 m curves. Note that the maximum discharge pressure is almost constant (about 22 bars in this example). This is consistent with the findings reported by Grant et al. (1982, pp. 138-139) and others, to the effect that the maximum discharge pressure depends only on the reservoir pressure and discharge enthalpy. Both of these parameters are constant in our analysis. For reservoirs with a lower permeability, the pressure drop in the reservoir becomes important, and a scaling law of the form given in equations (32) and (33) does not hold. For these cases, the production curves could be generated by solving equation (30) numerically for different values of p_{wh}.

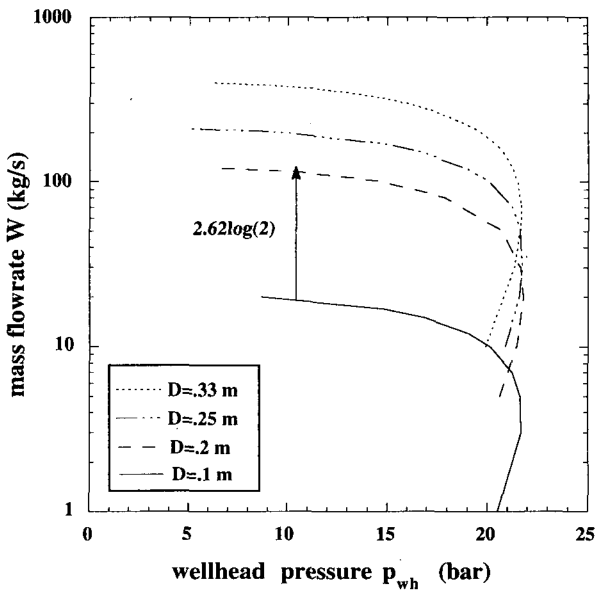

Fig. 4. Comparison of production of different diameter wells as a function of wellhead pressure. The curves are displaced vertically by an amount equal to $2.62\log(D/D_2)$.

APPLICATION TO FIELD DATA

In this example we use field measurements to test the scaling law analyses. Production well PW3-3 and slimhole TH#1 are located in the Steamboat Hills geothermal field, Nevada, and are about 15 m apart. They have been drilled to similar total depths, and hence probably extend through similar geological structure. Data for both wells (from Goranson, 1993) are shown in Table 2.

Since both wells are located in a highly permeable reservoir, the production rates should be controlled by the wellbore. Thus, it seems appropriate to use the scaling law given by equation (20). To use the scaling law, the production data for both wells have to be similar, except for diameters and mass flowrates. However, in this case the wellhead pressures for the two wells are not equal. In order to apply the scaling laws to these data, we proceed as follows. Since static and flowing pressure and temperature profiles are available for TH#1, we first calculated the productivity index. Using equation (2) and the data in Table 2, the calculated value was PI = 8.339×10^{-11} m^3. Then using the calculated productivity index the, wellbore simulator WFSA (Hadgu and Freeston, 1990) was used to predict mass flowrate for well TH#1 at a wellhead pressure of 3.97 bars. Additional input data for wellbore simulation were obtained from Table 2, and a roughness value of $\varepsilon = 4.5 \times 10^{-5}$ m was selected. The computed values using the wellbore simulator were W = 2.07 kg/s and p_{wb} = 22.78 bars. To predict the mass flowrate of the production well PW3-3, we used the scaling law given by equation (20):

$$W_1 = W_2 \left[\frac{D_1}{D_2} \right]^{2.5 - [\ln(2\varepsilon/D2)]^{-1}} \quad (34)$$

For $\varepsilon = 4.5 \times 10^{-5}$ m, $D_1 = 0.318$ m, $D_2 = 0.076$ m and $W_2 = 2.07$ kg/s, equation (34) gives $W_1 = 91.6$ kg/s. The measured flowrate to well PW3-3 was about 84.2 kg/s, which is 8.8% less than the value predicted by the scaling law. Although this is not a direct verification of the utility of the scaling law, this agreement is encouraging, considering the assumptions made in the analysis, and the unavoidable inaccuracies in the measured data.

Table 2: Data on wells PW3-3 and TH#1, Steamboat Hills (from Goranson, 1993).

	PW3-3	TH#1
total depth z(m)	258.2	272.6
casing diameter D(m)	0.318	0.076
openhole diameter D(m)	0.311	0.070
wellhead pressure p_{wh} (bar abs.)	3.97	3.07
mass flowrate W (kg/s)	~ 84.2	3.13
static bottomhole pressure p_r (bar abs.)	22.83	-
flowing bottomhole pressure p_{wb} (bar abs.)	22.76	-
bottomhole temp. T_{wb} (°C)	166.1	162.8

CONCLUSIONS

Analytical and numerical approaches to the characterization of output of different diameter geothermal wells have been presented. It is shown that flow processes in the reservoir and wellbore can be characterized by using scaling laws. The wellbore simulator WFSA (Hadgu and Freeston, 1990) was also used to provide numerical results to study flow processes when pressure drop in both the reservoir and wellbore are important. Future analysis should also include a study of the effect of wellbore heat losses to the formation. These studies need to be augmented with field data on slimholes and production size wells. Also, other topics concerning slimholes, such as well testing methodology, need to be studied to provide the basis for more effective use of slimholes.

ACKNOWLEDGMENTS

This work was supported by the Assistant Secretary for Energy Efficiency and Renewable Energy, Geothermal Division, U.S. Department of Energy under Contract No. DE-AC03-76SF00098, and through a sub-contract with Sandia National Laboratories. The authors appreciate the careful technical review of this report by Marcelo Lippmann and Akhil Datta Gupta of LBL, and thank Judith Peterson of LBL for help in the preparation of the manuscript. They also thank Far West Capital, Inc., for allowing the use of their field data.

REFERENCES

Aziz, K. and Settari, A. (1979), *Petroleum Reservoir Simulation*, Elsevier Applied Science Publishers, London.

de Marsily, G. (1986), *Quantitative Hydrogeology*, Academic Press, San Diego, Calif.

Entingh, D., and Petty, S. (1992), "Effects of Slim Holes on Hydrothermal Exploration Costs", *Geothermal Resourc. Counc. Trans.*, *16*, 73-81.

Grant, M.A., Donaldson, I., and Bixley, P. (1982), *Geothermal Reservoir Engineering*, Academic Press, New York.

Hadgu, T. (1989), "Vertical Two-Phase Flow Studies and Modelling of Flow in Geothermal Wells", *Ph. D. Thesis*, University of Auckland, New Zealand.

Hadgu, T. and Freeston, D.H. (1990), "A Multi-Purpose Wellbore Simulator", *Geothermal Resourc. Counc. Trans.*, *14*, 1279-1286.

Hadgu, T., Zimmerman, R.W., and Bodvarsson, G.S. (1993), "Coupling of a Reservoir Simulator and a Wellbore Simulator for Geothermal Applications", *Geothermal Resourc. Counc. Trans.*, *17*, 499-505.

Goranson, C. (1993), "Steamboat Hills Geothermal Field, Far West Capital, Inc., SB II and SB III Power Plants Lease Area Data Package", unpublished report, v. 1 to 3.

Gunn, C. and Freeston, D. H. (1991), "Applicability of Geothermal Inflow Performance and Quadratic Drawdown Relationships to Wellbore Output Curve Prediction", *Geothermal Resourc. Counc. Trans.*, *15*, 471-475.

Iglesias, E.R., and Moya, S.L. (1990), "Geothermal Inflow Performance Relationships", *Geothermal Resourc. Counc. Trans.*, *14*, 1201-1205.

Kjaran, S. P., and Eliasson, J. (1983), "Geothermal Reservoir Engineering Lecture Notes", *Report 1983-2*, U.N. Univ. Geothermal Training, Iceland.

Matthews, C.S., and Russell, D.G. (1967), *Pressure Buildup and Flow Tests in Wells*, Society of Petroleum Engineers, Richardson, Texas.

Pritchett, J. W., and Garg, S. K. (1980), "Determination of Effective Wellblock Radii for Numerical Reservoir Simulations", *Water Resourc. Res.*, *16(4)*, 665-674.

Pritchett, J.W. (1993), "Preliminary Study of Discharge Characteristics of Slim Holes Compared to Production Wells in Liquid-Dominated Geothermal Reservoirs", *Proc. 18th Workshop Geothermal Reservoir Engineering,* Stanford Univ., Stanford, Calif.

Pruess, K. (1987), "TOUGH User's Guide", *Report LBL-20700,* Lawrence Berkeley Laboratory, Berkeley, Calif.

White, F.M. (1974), *Viscous Fluid Flow*, McGraw-Hill, New York.